Putative Interhelix Ion Pairs Involved in the Stability of Myoglobin†

Carlos H. I. Ramos, Michael S. Kay, and Robert L. Baldwin*

Department of Biochemistry, Beckman Center, Stanford University Medical Center, Stanford, California 94305-5307

Received December 4, 1998; Revised Manuscript Received May 27, 1999

ABSTRACT: An earlier theoretical study predicted that specific ion pair interactions between neighboring helices should be important in stabilizing myoglobin. To measure these interactions in sperm whale myoglobin, single mutations were made to disrupt them. To obtain reliable ΔG values, conditions were found in which the urea induced unfolding of holomyoglobin is reversible and two-state. The cyanomet form of myoglobin satisfies this condition at pH 5, 25 °C. The unfolding curves monitored by far-UV CD and Soret absorbance are superimposable and reversible. None of the putative ion pairs studied here makes a large contribution to the stability of native myoglobin. The protein stability does decrease somewhat between 0 and 0.1 M NaCl, however, indicating that electrostatic interactions contribute favorably to myoglobin stability at pH 5.0. A previous mutational study indicated that the net positive charge of the A[B]GH subdomain of myoglobin is an important factor affecting the stability of the pH 4 folding intermediate and potential ion pairs within the subdomain do not contribute significantly to its stability. One of the assumptions made in that study is tested here: replacement of either positively or negatively charged residues outside the A[B]GH subdomain has no significant effect on the stability of the pH 4 molten globule.

Pairs of oppositely charged residues on adjacent helices are predicted to make strong electrostatic interactions in sperm whale Mb[1] (*1*). These interactions are predicted to be screened by counterions although, if they are present as salt bridges (hydrogen-bonded ion pairs), these are not found to be very sensitive to counterion screening, in peptide helices (*2, 3*). In either case, if there are any strong pairwise interactions between oppositely charged residues on adjacent helices**,** they are likely to be important in determining the folding pathway of apoMb. We undertook to measure them, to find out if any changes in stability are indeed caused by pairwise interactions, and to determine how the stability of Mb is affected by counterion screening.

Our procedure is to substitute by alanine at least one member of each potential ion pair and to determine the resulting change ($\Delta\Delta G$) in its free energy of unfolding (ΔG_{unf}). If replacing one residue gives a significant change in ΔG_{unf}, then the other residue of the pair is substituted with alanine and $\Delta\Delta G$ is measured to find out if the second mutation causes an equally large change, as expected if there is a pairwise interaction. The test for a pairwise interaction is essential when mutation of one member of a pair gives a large change in stability because other effects, such as steric, hydrophobic, or helix propensity effects, may be responsible for the observed change. To obtain reliable $\Delta\Delta G$ values, the folding transition must be reversible and two-state. We searched for conditions in which the urea-induced unfolding of holoMb satisfies this condition. GdmCl is unsatisfactory for this purpose because high Cl^- concentrations stabilize a folding intermediate. We found that the cyanomet form of holoMb gives reversible, two-state, urea-induced unfolding at pH 5.0, 25 °C. Urea unfolding of native apoMb at pH 7.8, 4 °C, has been used earlier (*5*) to study the effects of mutations on the stability of native apoMb, but for mutants it is often necessary to use a three-state analysis, which gives less accurate results than the new two-state procedure introduced here. For technical reasons, the new procedure is limited to pH values close to 5.0 (see below).

The contribution of electrostatic free energy (ΔG_{el}) to ΔG_{unf} *is* predicted to be large and favorable for Mb folding at pH 7, where there are similar numbers of positively and negatively charged groups, using either the accessibility-modified Tanford−Kirkwood model (*1*) or the finite difference Poisson−Boltzmann (FDPB) procedure (*4*). Both models also predict that ΔG_{el} should become large and unfavorable at pH 2, where the net positive charge is large. At pH 7.0, ionic strength 0.01, ΔG_{el} for Mb is predicted to be near −18 kcal/mol. There are few experimental tests in the literature of the size of ΔG_{el} as it affects protein stability. Hollecker and Creighton (*6*) made one such test by reversing the basic charges on amino groups through succinylation. They found only small effects of net charge on stability, measured by urea-gradient gel electrophoresis, for β-lactoglobulins A and B, cytochrome *c*, and ribonuclease A, although succinylation of a single unreactive amino group of cytochrome *c* did produce a substantial decrease in stability. They used an acidic pH (4.0) in determining the

† This work was supported by NIH Grant GM 19988. C.H.I.R. is a PEW Latin American Fellow (P0195SC) and was also supported by FAPESP (96/06919-9). M.S.K. is a trainee of the National Institute of General Medical Sciences Medical Scientist Training Program.

* Corresponding author. Phone: (650) 723-6168. Fax: (650) 723-6783. E-mail: bbaldwin@cmgm.stanford.edu.

[1] Abbreviations: Mb, myoglobin; CD, circular dichroism; I, pH 4 folding intermediate; N, native; C_m, urea concentration where the protein is 50% folded; ΔG_{unf}, free energy of unfolding; ΔG_{el}, electrostatic free energy; T_m, the temperature midpoint of a thermal unfolding curve; GdmCl, guanidinium chloride.

10.1021/bi9828627 CCC: $18.00
Published on Web 07/09/1999

Table 1: Predicted Electrostatic Interactions between Pairs of Mb Residues Studied in this Paper[a]

paired residues ($i-j$)	adjacent helices[b]	$\Delta\Delta G_{ij}$[c]	r_{ij}[d]	SA[e] (i, j)
Glu04−Lys79	A−EF	−1.49	2.73	0.20, 0.50
Glu06−Lys133	A−H	−1.15	2.83	0.50, 0.45
Lys16−Asp122	A−GH	−1.21	3.38	0.05, 0.60
Glu18−Lys77	A−E	−1.21	2.97	0.30, 0.55
Asp20−Arg118	B−G	−1.17	3.28	0.50, 0.25
Asp44−Lys47	CD−CD	−0.93[f]	3.24	0.45, 0.55
Arg45−Asp60	CD−E	−1.72	3.05	0.15, 0.15
Glu52−Lys56	D−D	−1.26[f]	2.98	0.45, 0.35
Glu105−Arg139	G−H	−0.78	4.52	0.30, 0.40

[a] The data are from Garcia-Moreno et al. (*1*); this table is similar to Table 4 in that paper. [b] Position of the residues in Mb: helix (one letter) or turn (two letters). [c] Free energy values are given in kcal/mol at pH 7.0 and 0.01 M ionic strength (*1*). [d] r is the distance between atoms in Å. [e] SA is fractional static solvent accessibility of the charged atom (varies from 0.05 for totally buried to 0.95 for completely solvent-exposed) (*1*). [f] Average of the intraelement values for the two residues (from Table 1 of ref 1).

effect of charge reversal on the stability of cytochrome *c* and ribonuclease A; because pH 4.0 is close to the pH range where the predicted values of ΔG_{el} change from negative to positive, they may have found small effects only for this reason. Meeker et al. (*7*) replaced each of the ionizable residues of staphylococcal nuclease and found only small effects on stability in general, although a few mutations did cause a large decrease in stability, about 3 kcal/mol. Previous mutational studies of specific ion pairs in proteins are discussed below.

EXPERIMENTAL PROCEDURES

Protein Expression and Purification. Mutations were constructed using a cloned sperm whale Mb cDNA (*8*). The expression and purification of recombinant Mb were as described in Loh et al. (*9*). ApoMb was prepared as described in Rossi-Fanelli et al. (*10*) and its concentration determined as described by Edelhoch (*11*). The mutations were made and confirmed by DNA sequencing at the Stanford Protein and Nucleic Acid facility. The mutants made were E04A, E18A, K77A, D44A, K56A, and D60A. The recombinant proteins were expressed in high levels and shown to be more than 95% pure by SDS polyacrylamide-gel electrophoresis (*12*). The net charge difference between wild-type apoMb and mutants was confirmed by nondenaturant polyacrylamide gel electrophoresis at pH 9.0 (data not shown). Production of the other Mb mutants studied here (H24V/H119F, D20A, R118A, R122A, K133A, and K139A) is described elsewhere (*13*, *14*). The mutants made and their potential pairwise interacting partners are shown in Table 1.

CyanoMb Preparation. Cyanoheme stock solutions were prepared by mixing bovine hemin (Sigma) and KCN (Mallinckrodt) to a final concentration of 2.3 and 77 mM, respectively, at pH 10. CyanoMb, Mb with cyanoheme, was prepared by mixing on ice apoMb with the cyanoheme solution in a 1:1 ratio of protein to hemin; for some mutants the mixed solution was allowed to equilibrate for days in order to improve the formation of cyanoMb. After preparation, the protein was ultracentrifuged at 90 000*g* for 10 min at 4 °C in a Beckman TL-100 ultracentrifuge. The supernatant was collected and the concentration measured spectrophotometrically using the following extinction coefficients: 423 nm, 109.7 cm^{-1} mM^{-1}, and 280 nm, 35 cm^{-1} mM^{-1}, in 50 mM Tris, pH 7.0 (*15*). The protein was used in further experiments if the concentration values measured at the two wavelengths varied by less than 10%.

Denaturation Conditions. Urea solutions were prepared freshly and filtered. The concentration of the solution was measured by its refractive index as described by Pace (*16*). The cyanoMb experiments were carried out at 10 mM Na acetate in the pH range between 4.0 and 6.0 (pH adjusted with HCl), 0.5 mM KCN, at 25 °C. CyanoMb unfolding reached equilibrium within 1 h after dilution into denaturant. Wild-type refolding at pH 5.0 was carried out by diluting cyanoMb in 10 M urea and then by diluting to a lower urea concentration before CD measurement. H24V/H119F refolding at pH 4.0 was carried out by diluting the protein in 8 M urea. Experiments with the pH 4 folding intermediate were made in 4 mM citrate, pH 4.2, 4 °C, and were allowed to equilibrate for 20 min after dilution into denaturant.

Spectrophotometric Measurements. The CD measurements were made with an Aviv 62A-DS spectropolarimeter with a 1 cm path length cuvette at 222 nm. Concentrations were 1 μM for cyanoMb and 2 μM for apoMb. Soret absorbance was measured on a Beckman DU640 spectrophotometer at 423 nm using a 1 cm path length cuvette with 2 μM cyanoMb. Fluorescence data were taken on a SLM AB2 spectrofluorimeter using a 1 × 1 cm path length cuvette with 2 μM apoMb. Excitation was at 288 nm with a band-pass of 2 nm, and emission was measured at 320 nm with a band-pass of 8 nm. A wild-type urea-induced unfolding curve was reproduced during each set of experiments with mutants in order to test if the conditions were reproducible.

Data Analyses. Urea-induced unfolding curves were fitted to a two-state equation as described by Santoro and Bolen (*17*). The curves were fitted with KaleidaGraph (Abelbeck software). All analyses of cyanoMb wild-type or mutant curves were made using the *m* value obtained for the wild type at pH 5.0 in the absence of NaCl. For the pH 4 folding intermediate, the *m* value and native baseline of the wild-type apoMb intermediate were used to fit the mutant fluorescence data, since the baselines for many mutants could not be determined accurately.

RESULTS

Urea-Induced Unfolding of cyanoMb and apoMb. Figure 1 shows urea-induced unfolding of wild-type cyanoMb followed by two different probes, CD at 222 nm and absorbance at the Soret band (423 nm). The raw data are shown in Figure 1a, and the fraction folded is shown in Figure 1b. Unfolding followed either by CD or by absorbance at the Soret band shows identical transition curves characteristic of two-state unfolding. Unfolding under these conditions is reversible (Figure 1b). The unfolding curves of cyanoMb and apoMb at pH 5.0 are shown in Figure 2. ApoMb unfolds at a lower urea concentration than cyanoMb in the same conditions.

Data Analysis. The cyanoMb mutant unfolding curves are analyzed using the *m* value obtained for the wild type at pH 5.0, 25 °C, in the absence of salt: 1.6 kcal mol^{-1} M^{-1}. Using this approach, we can relate the unfolding free energies of mutant and wild type by comparing the C_m values: *m*-value determinations are not very accurate for technical reasons

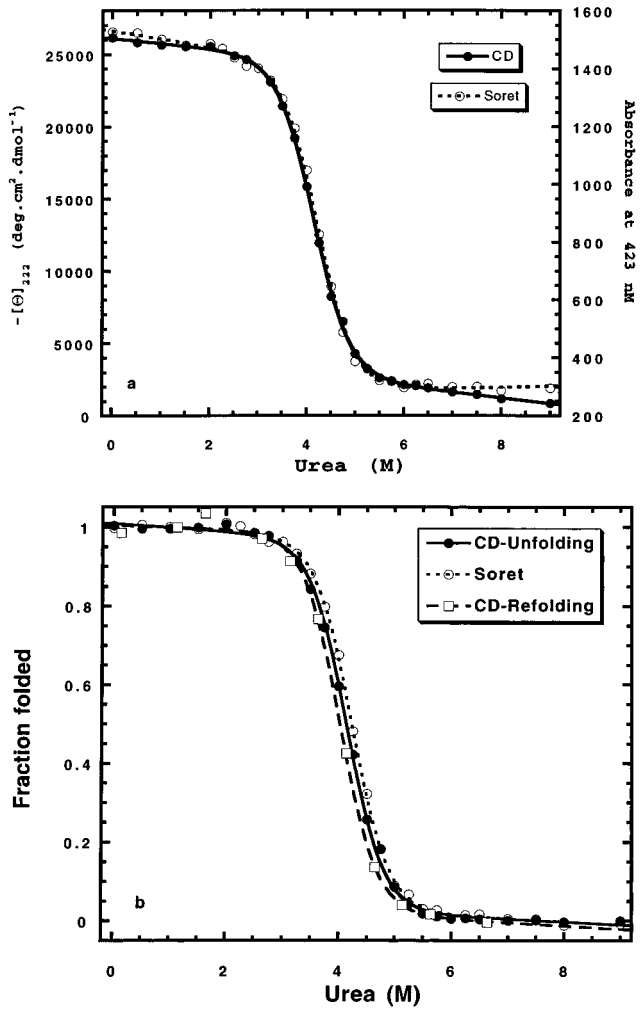

FIGURE 1: Urea-induced unfolding of cyanoMb at pH 5.0, 25 °C, followed by two different probes is two-state and reversible. (a) CD measurements at 222 nm, a secondary structural probe, and absorbance at the Soret band (423 nm), a tertiary structural probe, are plotted as a function of urea concentration. The measured values are shown by symbols and the fitted curves by lines. (b) Normalized fraction folded, measured by CD at 222 nm and by absorbance at the Soret band (423 nm), are plotted as a function of urea concentration, both for unfolding and refolding.

(*18*). In the analysis of the unfolding curves of the pH 4 folding intermediate, using fluorescence data, the same approach is used. The urea unfolding curves of I for mutants are analyzed using the *m* value obtained for wild type: 1.83 kcal mol^{-1} M^{-1}. The wild-type folded baseline is also used to fit the mutant data. These baselines are not determined accurately because of an increase in fluorescence well below the transition zone. For the wild type this effect occurs because of an urea-dependent equilibrium between two forms of the folding intermediate (Ia and Ib) at low urea concentrations (<1 M) (*19*).

Stability of cyanoMb Native State. Figure 3 shows the raw data (a) and fraction folded (b) for urea-induced unfolding of the wild type and representative charged-site mutants of cyanoMb measured by CD. Wild-type cyanoMb has C_m = 4.2 M urea (Table 2). Table 2 gives the urea midpoint and $\Delta\Delta G$ for urea-induced unfolding of wild type and mutants, measured by CD and Soret absorbance. The predicted values of $\Delta\Delta G$ for the potential salt bridge mutants (*1*) are also given in Table 2. The results obtained by Soret absorbance

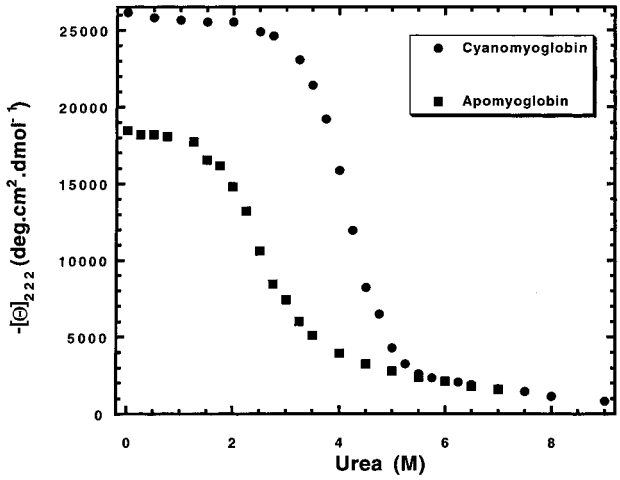

FIGURE 2: ApoMb unfolds at a lower urea concentration than cyanoMb at pH 5.0 and 25 °C. CD measurements at 222 nm are plotted as a function of urea concentration.

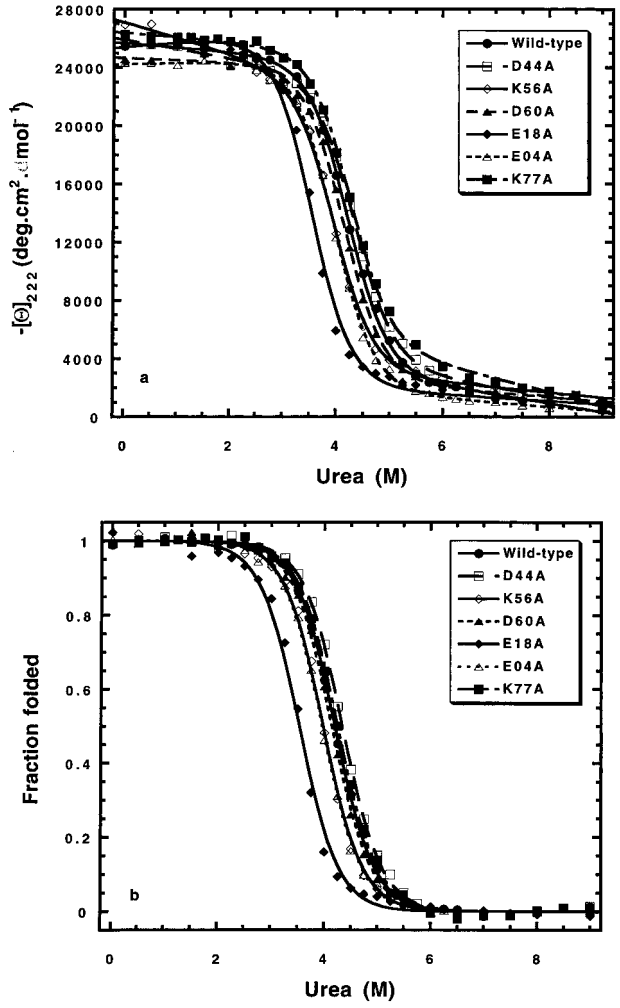

FIGURE 3: Urea-induced unfolding of cyanoMb at pH 5.0 for charged-site mutants. The CD measurements at 222 nm (a) and the normalized fraction folded (b) are plotted as a function of urea concentration. The parameters obtained from the data analysis are given in Table 2.

are in good agreement with the ones obtained by CD (Table 2). One pairwise interaction is found: Asp20−Arg118. Each of the single mutants gives $\Delta\Delta G = -0.5$ kcal mol^{-1}. Replacement of Glu18 by Ala gives $\Delta\Delta G = -1.0$ kcal mol^{-1}, but replacement of Lys77 by Ala gives only $\Delta\Delta G =$

Table 2: Free Energy of Unfolding for Mb Mutants at Charged Sites: Experimental and Predicted Values

paired residues[a]	C_M[b] (CD, Soret)	$\Delta\Delta G$:[c] CD, Soret	$\Delta\Delta G_{ij}$:[c,d] predicted
wild type	4.19, 4.21	0, 0[e]	
Glu04−Lys79	3.97, 3.81	−0.35, −0.65	−1.49
Glu06−***Lys133***	4.16, 4.28	−0.05, +0.10	−1.15
Lys16−***Asp122***	4.13, 4.20	−0.10, −0.05	−1.21
Glu18 - Lys77	3.59, 3.53	−0.95, −1.10	−1.21
Glu18−***Lys77***	4.31, 4.34	+0.20, +0.20	−1.21
Asp20−Arg118	3.87, 3.97	−0.50, −0.40	−1.17
Asp20−***Arg118***	3.78, 3.81	−0.65, −0.65	−1.17
Asp44−Lys47	4.34, 4.25	+0.25, +0.05	−0.93
Arg45−***Asp60***	4.13, 4.06	−0.15, −0.25	−1.72
Glu52−***Lys56***	3.97, 4.06	−0.35, −0.25	−1.26
Glu105−***Arg139***	3.91, 3.94	−0.45, −0.45	−0.78

[a] The pair of mutated residues is shown, and the mutated residue is in bold type and italicized. [b] C_m is the molar urea concentration at 50% folded. [c] $\Delta\Delta G = \Delta G$(wild type) − ΔG(mutant); values given in kcal/mol. [d] Prediction made by Garcia-Moreno et al. (*1*). [e] The free energy of unfolding for the wild type is −6.70 kcal/mol by CD and −6.75 kcal/mol by Soret absorbance.

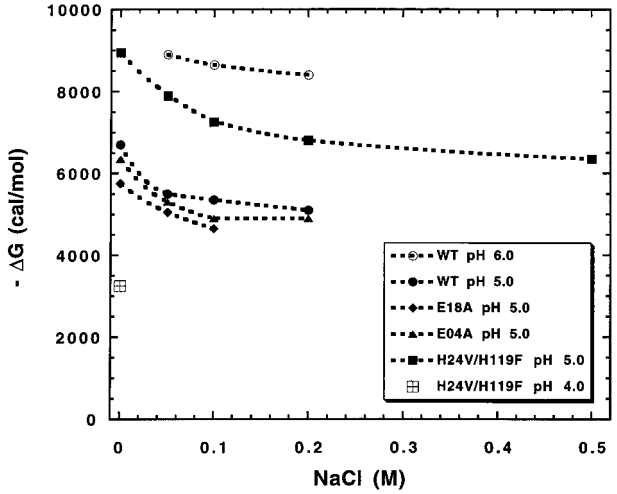

FIGURE 4: Salt dependence of ΔG for the urea-induced unfolding of cyanoMb, showing how the stability depends on pH and [NaCl]. Dashed lines are used only to link the symbols and have no further meaning.

0.2 kcal mol^{-1}, so that Glu18−Lys77 is not a strong pairwise interaction. In the X-ray structure of Mb (*20*), Glu 18 makes a hydrogen bond to the indole NH of Trp 14, which may explain the destabilizing effect of E18A. Several other mutants give $\Delta\Delta G$ values of −0.2 kcal mol^{-1} or less (D44A, D60A, D122A, and K133A), and a few mutants give $\Delta\Delta G$ values in the range −0.2 to −0.5 kcal mol^{-1} (K56A, E04A, and K139A).

Dependence of Stability on [NaCl]. Figure 4 shows the unfolding free energy of wild-type (pH 5.0 and 6.0) and mutant (pH 5.0 and 4.0) cyanoMb as a function of [NaCl]. There is an increase in stability for wild-type cyanoMb as the pH increases from pH 5.0 to pH 6.0, and there is a decrease in stability as [NaCl] increases. The wild-type stability measurements at pH 4.5 indicate a deviation from two-state behavior (data not shown).

The double mutant H24VH119F is also studied here (Figure 5) because apoMb remains native at pH 4 with this mutant, unlike the wild type. The stability of H24V/H119F decreases as the pH decreases from 5.0 to 4.0, and there is a decrease in stability with increasing [NaCl] (Figure 5). Most

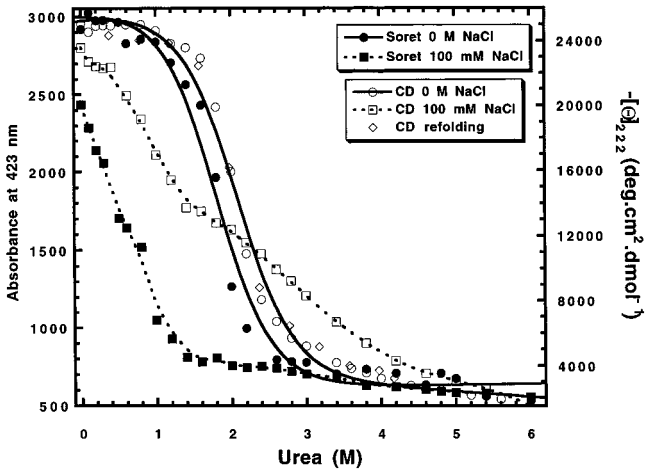

FIGURE 5: Salt dependence of the urea-induced unfolding of H24V/H119F cyanoMb at pH 4.0. CD measurements at 222 nm and absorbance at the Soret band (423 nm) are plotted as a function of urea concentration. The measured values are shown by symbols, and the fitted curves, by solid lines. Dashed lines are used only to link the symbols and have no further meaning. The presence of NaCl causes a loss of the Soret signal and formation of apoMb when H24V/H119F cyanoMb unfolds at pH 4.0.

of the decrease in stability occurs at low salt concentration (less than 50 mM), both for wild-type and mutant cyanoMb (Figure 4). Figure 5 shows the urea-induced unfolding of H24V/H119F at pH 4.0 at 0 and 100 mM NaCl. The raw data (CD and Soret absorbance) are shown in order to compare the different behavior revealed by these two probes. Comparison of the CD and Soret data at 0 M NaCl shows some deviation from two-state unfolding. At 100 mM NaCl the deviation is large and the Soret results suggest a substantial loss of stability. Both CD and Soret absorbance data show slightly reduced signals at 0 M urea. Similar results are seen in 50 mM NaCl (data not shown). The urea-induced unfolding of H24V/H119F is reversible at 0 M NaCl, pH 4.0.

Stability of the pH 4 Intermediate. Figure 6 shows the fraction folded, as monitored by CD, for urea-induced unfolding of the pH 4 folding intermediate, for wild type and mutants. Table 3 shows C_m and $\Delta\Delta G$, measured both by CD and fluorescence. The wild-type pH 4 intermediate has C_m = 1.58 M urea (Table 3). The results obtained by fluorescence are in good agreement with the ones obtained by CD (Table 3). The stability of the mutants D44A, K56A, K77A, and D60A is similar to the wild type. Mutants E04A and E18A are less stable than the wild type. Data for D20A, R118A, D122A, K133A, and R139A were given earlier (*14*): R118A, K133A, and R139A increase the stability of I, while both D20A and D122A give no conclusive change in stability.

DISCUSSION

The objective of our work is to determine whether specific ion pair interactions make an important contribution to the stability of Mb, as suggested by the electrostatic predictions of Garcia-Moreno et al. (*1*), based on the accessibility-modified Tanford−Kirkwood model. To undertake this study, we first found conditions in which the urea-induced unfolding of holoMb is two-state and reversible, namely with cyanoMb at pH 5.0.

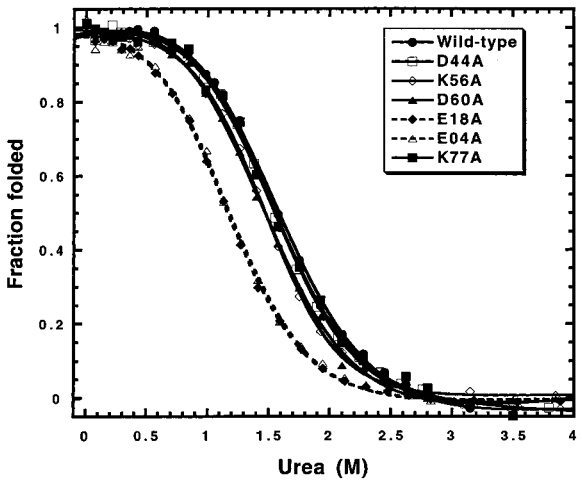

FIGURE 6: Replacement of negatively charged residues by alanine in the AGH subdomain destabilizes the pH 4 folding intermediate. The normalized fraction folded, measured by CD at 222 nm, is plotted as a function of urea concentration. Unfolding was measured up to 5.6 M urea, but only the results between 0 and 4 M are shown. The measured values are shown by symbols and the fitted curves by lines, and the parameters obtained from the data analysis are given in Table 4.

Table 3: Free Energy of Unfolding of the pH 4 Folding Intermediate (I) for New Charged Site Mutants Not Studied Previously (See Ref *14*)

I	C_M[a] (CD, fluorescence)	$\Delta\Delta G$[b] (CD, fluorescence)
wild type	1.58, 1.50	0, 0[c]
D44A	1.50, 1.40	−0.15, −0.20
K56A	1.45, 1.40	−0.25, −0.20
D60A	1.53, 1.42	−0.10, −0.15
E18A	1.20, 1.23	−0.70, −0.50
E04A	1.20, 1.20	−0.70, −0.55
K77A	1.56, 1.50	−0.05, −0.02

[a] C_m is the molar urea concentration at 50% folded. [b] $\Delta\Delta G = \Delta G$(wild type) − ΔG(mutant); values given in kcal/mol. [c] The free energy of unfolding for the wild type is −2.90 kcal/mol by CD and −2.75 kcal/mol by fluorescence.

Use of Urea-Induced Unfolding of cyanoMb at pH 5.0 To Measure Stability. To determine if unfolding is two-state, we compare the unfolding transition curves monitored by two probes, one of secondary structure (far-UV CD at 222 nm) and one of tertiary structure (Soret absorbance). For urea-induced unfolding at pH 5.0, 25 °C, even the raw data, without baseline correction, show good superposition of the two unfolding curves (Figure 1a). Also, the steepness of the transition curve shows that unfolding is highly cooperative. The reversibility of unfolding in these conditions is good (Figure 1b), provided that adequate time is allowed to reach equilibrium. Slow equilibration is caused by heme dissociation after unfolding. Poor reversibility is caused by heme stacking. This is prevented by using the cyanomet form of Mb. At 3 M urea, pH 5.0, where cyanoMb begins to unfold (Figure 2), apoMb is almost completely unfolded and cyanoMb is much more stable than apoMb in these conditions. This is important in bringing about two-state unfolding of cyanoMb, because native apoMb would otherwise be a stable folding intermediate**.** The stability of cyanoMb increases rapidly as the pH is increased above 5. At pH 6.0, 25 °C, complete unfolding is obtained only in 10 M urea, and at pH 7.8 cyanoMb is only partially unfolded in 10 M urea (data not shown). On the other hand, at pH 4.5 unfolding of cyanoMb is no longer two-state (data not shown). These considerations limit our study of wild-type cyanoMb to pH 5.0. The double mutant H24V/H119F, which does not form a folding intermediate at pH 4.0 (*21*), can be studied at pH 4.0, at 0 M NaCl, where its cyanoMb form shows two-state unfolding (Figure 5).

Hargrove and Olson (*22*) point out that, at sites where mutations contact the heme group, the stability of holoMb is determined chiefly by the affinity of apoMb for heme. The mutations studied here all involve replacement of a charged residue by alanine, and these sites do not contact the heme. Moreover, the mutations affect the stability of native apoMb and holoMb (cyanoMb) in a similar manner (pH and urea-induced unfolding curves of native apoMb not shown).

Using C_m Values To Measure Relative Stability of Mutants. In Tables 2 and 3 we follow the procedure of Johnson and Fersht (*18*) in calculating $\Delta\Delta G$ for mutants from their C_m values by using the *m* value for wild type. As they point out, the C_m values can be measured more precisely than the *m* values, and if the conventional interpretation of the *m* value is adopted (*m* is proportional to the buried surface area exposed on unfolding), then *m* values are not expected to vary significantly in a series of point mutants unless the amount of buried surface area in the denatured ensemble can be changed by point mutations. Shortle and co-workers (*23*) have shown that point mutations do affect the apparent *m* values of staphylococcal nuclease (SNase) mutants, and they attribute the changes to the denatured ensemble. It is controversial, however, whether SNase and these mutants show two-state, or more complex, unfolding behavior (24−27) and whether the mutational changes in *m* values may in fact reflect deviations from two-state behavior. By size exclusion chromatography, Baskakov and Bolen (*27*) have shown recently that one of Shortle's mutants (V66W) deviates from two-state behavior and that the properties of the denatured ensemble of SNase are complex ("variable"), in contrast to those of RNase A whose properties are "fixed" as a denatured ensemble.

Our results do not suggest that there are significant mutant-specific changes in the *m* value when the stability of holoMb is measured. The urea unfolding curves (Figure 1) satisfy standard tests for two-state folding: the curves are symmetrical and reversible, and the two curves monitored by probes of secondary structure (far-UV CD) and tertiary structure (Soret absorbance) are superimposable. Thus, it is plausible that cyanoMb represents a well-behaved two-state system like RNase A rather than a more complex system like SNase, but future work is needed to decide this point. The results presented here for the pH 4 folding intermediate of apoMb also satisfy a standard test for two-state folding: the unfolding curves monitored by probes of secondary structure (far-UV CD) and tertiary structure (tryptophan fluorescence) are superimposable. However, earlier work showed that severely destabilizing mutations cause a breakdown of two-state folding (*28, 29*) and this caveat should be remembered. The charged site mutants studied here cause only moderate changes in stability of the intermediate.

The Potential Ion Pairs Studied Here Make Little Contribution to the Stability of cyanoMb. Of the nine potential ion pairs studied here, most of which were predicted (*1*) to

stabilize Mb by more than 1 kcal mol^{-1} (Table 1), only one pairwise interaction (Asp20−Arg118) was found to stabilize Mb by as much as 0.5 kcal mol^{-1}. The residues studied here are chiefly solvent exposed (*1*), and for that reason, not much change in stability might be expected as a result of mutating them. Nevertheless, they were predicted to be stabilizing (*1*). The nine potential ion pairs include several interhelix candidates (Table 1) which, if they had been found, might have proven important in determining the folding pathway of apoMb. Two other replacements of a charged residue by alanine (Glu4 and Arg139) gave almost a 0.5 kcal mol^{-1} decrease in stability, and they remain possible candidates for minor pairwise interactions. The stabilizing effects of the mutations made here were tested at pH 5.0 for reasons explained above, but the predicted interhelix interactions were evaluated at pH 7.0 (1). The overall electrostatic interactions of these residues were predicted, however, both at pH 5.0 and at pH 7.0 (see Table 1 of ref *1*), and the interhelix interactions account for the major part of the overall electrostatic interactions. The predicted overall interactions change only slightly between pH 5.0 and pH 7.0, which suggests that the results found here may also be applicable at pH 7.0.

These results suggest that the accessibility-modified Tanford−Kirkwood model overestimates the actual electrostatic interactions in proteins, for a reason that remains to be determined. The current FDPB procedure also overestimates electrostatic effects when used to predict pK_a values in proteins (*30*). The best agreement with actual pK_a values is obtained by using a fictitious value of 20 for the dielectric constant rather than a more realistic value of 4. This is equivalent to saying that the actual electrostatic interactions in proteins are 5 times weaker than predicted. A possible solution to the puzzle has been offered by Havranek and Harbury (unpublished results). They use a dielectric constant of 4 and allow the rigid side chains of the X-ray structure to relax in response to electrostatic stress. Their procedure, which combines elements of the Tanford−Kirkwood model and the FDPB procedure, gives somewhat better prediction of pK_a values than a dielectric constant of 20 used with rigid side chains. Possibly their procedure would give predicted electrostatic interactions in Mb that agree better with the experimental values given here in Table 2.

Other Tests of Ion Pairs Involved in the Stability of Proteins. A specific pairwise His−Asp interaction makes a major contribution (3−5 kcal mol^{-1}) to the stability of T4 lysozyme (*31*), as judged both by the pK_a shifts of the His and Asp residues involved and by the effects on ΔG_{unf} of mutating either the His or the Asp residue to Asn. Similarly, an Asp−Arg interaction makes a major contribution to the stability of barnase (*32*). On the other hand, Arc repressor contains a complex ion pair interaction involving three partially buried charged side chains and replacement of all three charged residues by nonpolar residues increases its stability (*33*). Side chain ion pairs, at specific spacings of i, $i + 4$, stabilize peptide helices by modest but measurable amounts (*3*, *4*). They are salt bridges (hydrogen-bonded ion pairs) in which the hydrogen bond is a major contributor to stability, as judged both by the effects of protonating carboxylate groups and by attempting to screen the interaction with NaCl. A complex RER salt bridge significantly stabilizes the GCN4 dimeric coiled coil (*34*), and the RER residues are expected to be solvent exposed. Complex networks of ionized side chains are commonly found on the surfaces of thermophilic proteins, but evaluation of their stabilizing effects is still under discussion (*35*).

Decrease of Mb Stability with increasing [NaCl] and at Acid pH. The results shown in Figure 4, in which ΔG_{unf} decreases significantly as [NaCl] increases from 0 to 0.1 M, demonstrate directly that favorable electrostatic interactions contribute to the stability of Mb at these pHs. The decrease in ΔG_{unf} is not large (about 2 kcal mol^{-1}), but it is significant in comparison with the value of ΔG_{unf} itself, which varies from about 3 to 9 kcal mol^{-1} in Figure 4, depending on the pH and the mutant studied as well as on [NaCl]. pH 5 should not be far from the pH where the net charge is zero and ΔG_{el} changes sign, from being unfavorable at low pH, where only positively charged groups are present, to being favorable at neutral pH, where both positive and negative charges are present. Consequently, if similar experiments could be made at higher pHs, larger effects of [NaCl] might well be found. Unfortunately, cyanoMb is too stable to permit urea unfolding experiments at higher pHs. The crossover pH where the net charge is zero must be measured, not calculated, because it depends on anion binding as well as on the distribution of acidic and basic residues in the protein; it can be measured by electrophoresis.

A strong decrease in ΔG_{unf} at acid pH is predicted by electrostatic calculations and is observed for almost all proteins; usually the decrease in stability is observed as T_m versus pH, where T_m is the temperature midpoint of a thermal unfolding curve. Direct measurements of ΔG_{unf} versus pH by urea or GdmCl unfolding have been made for a few proteins such as RNase A (*36*, *37*), and they confirm that there is a large decrease in ΔG_{unf} at acid pH. The pK_a values of all the carboxylate residues of T4 lysozyme have been measured by NMR and used to predict the pH dependence of $\Delta G_{unf.}$ At pH 1 the predicted value of the pH-dependent contribution is very large, about 17 kcal/mol (*38*). These results are consistent with large unfavorable values of ΔG_{el} at acid pH, resulting from mutual repulsion between positively charged groups; however, some of the abnormally low pK_a values might arise from other causes, such as hydrogen bonding. His 24 in native apoMb is buried and H-bonded to His 119, and it is not detectably protonated in native apoMb, even at pH 4.0 (*21*). Its pK_a is below 3.0, but it is predicted to be 5.1 by a FDPB calculation (*4*).

Effects of Charged-Site Mutations on the Stability of the pH 4 Folding Intermediate. The partly folded form of apoMb found at pH 4 (I), which contains stable A, G, and H helices and a partly stable B helix, is unfolded by acid below pH 4, in a pH range where only Asp and Glu residues are protonated. An earlier study (*14*) considered two models for the acid-induced unfolding of I: a net charge mechanism, in which I unfolds when the electrostatic repulsion between positively charged residues exceeds a critical value as Asp and Glu residues become protonated, and a salt bridge mechanism, in which I unfolds when the salt bridges that stabilize I are broken as Asp and/or Glu residues become protonated. The two mechanisms have been tested by mutating the basic residues in the putative salt bridges to alanine. According to the salt bridge mechanism, these mutations should destabilize I. According to the net charge mechanism, they should stabilize I. Six basic residues (Lys,

Arg) within the A[B]GH subdomain were replaced singly, and each of them was found to stabilize I (*14*). Thus, the earlier results strongly support the net charge mechanism. Net charge, rather than ΔG_{el} calculated using a point charge model, was considered because a detailed structure of this folding intermediate is not available.

In the net charge model used to interpret the earlier results, only charged residues in the A[B]GH subdomain were considered. Charged residues outside this subdomain were treated as not contributing to the net charge. The results in Table 3 support this assumption because mutation to alanine of any of 4 charged residues outside the A[B]GH subdomain (D44, K56, D60, K77) has no effect on the stability of the folding intermediate. Moreover, mutation to alanine of either of two acidic residues (E4, E8) within the A[B]GH subdomain destabilizes I, consistent with the model. The acidic residues may be partly ionized at the pH (4.2) where the stability of I is measured, and mutation of an acidic residue may produce a smaller effect for this reason. Earlier, mutation to alanine of two aspartate residues (D20A, D122A) within the A[B]GH subdomain was found to have no effect on the stability of I (*14*). Changes in helix propensity are known to affect the stability of I (*28*), and because aspartate has a much lower helix propensity than alanine, the helix stabilizing effect of Asp → Ala may have compensated the net charge effect, which is destabilizing.

ACKNOWLEDGMENT

We thank Pehr Harbury, Marc Jamin, and Doug Laurents for discussion and suggestions. We also thank Dr. Jose Sanchez-Ruiz for a preprint of his paper (ref *39*, received after this manuscript was completed), which describes a procedure for experimentally quantitating the contributions of charge−charge interactions to protein stability.

REFERENCES

1. Garcia-Moreno, B., Chen, L. X., March, K. L., Gurd, R. S., and Gurd, F. K. N. (1985). Electrostatic interactions in sperm whale myoglobin. *J. Biol. Chem. 260*, 14070−14082.
2. Smith, J. S., and Scholtz, J. M. (1998). Energetics of polar side-chain interactions in helical peptides: salt effects on ions pairs and hydrogen bonds. *Biochemistry 37*, 33−40.
3. Huyghues-Despointes, B., and Baldwin, R. L. (1997). Ion-pair and charged hydrogen-bond interactions between histidine and aspartate in a peptide helix. *Biochemistry 36*, 1965−1970.
4. Yang, A.-S., and Honig, B. (1994). Structural origins of pH and ionic strength effects on protein stability. Acid denaturation of sperm whale myoglobin. *J. Mol. Biol. 237*, 602−614.
5. Kay, M. S., and Baldwin, R. L. (1996). Packing interactions in the apomyoglobin folding intermediate. *Nat. Struct. Biol. 3*, 439−445.
6. Hollecker, M., and Creighton, T. E. (1982). Effect on protein stability of reversing the charge on amino groups. *Biochim. Biophys. Acta 701*, 395−404.
7. Meeker, A. K., Garcia-Moreno, B., and Shortle, D. (1996). Contributions of the ionizable amino acids to the stability of staphylococcal nuclease. *Biochemistry 35*, 6443−6449.
8. Springer, B. A., and Sligar, S. G. (1987). High-level expression of sperm whale myoglobin in *Escherichia coli*. *Proc. Natl. Acad. Sci. U.S.A. 84*, 8961−8965.
9. Loh, S. N., Kay, M. S., and Baldwin, R. L. (1995). Structure and stability of a second molten globule intermediate in the apomyoglobin folding pathway. *Proc. Natl. Acad. Sci. U.S.A. 92*, 5446−5450.
10. Rossi-Fanelli, A., Antonini, E., and Caputo, A. (1958). Studies on the structure of hemoglobin. I. Physicochemical properties of human globin. *Biochim. Biophys. Acta 30*, 608−615.
11. Edelhoch, H. (1967). Spectroscopic determination of tryptophan and tyrosine in proteins. *Biochemistry 6*, 1948−1954.
12. Laemmli, U.K. (1970). Cleavage of structural proteins during the assembly of the head of bacteriophage T4. *Nature 277*, 680−685.
13. Barrick, D., Hughson, F. M., and Baldwin, R. L. (1994). Molecular mechanism of acid denaturation: The role of histidine residues in the partial unfolding of apomyoglobin. *J. Mol. Biol. 237*, 588−601.
14. Kay, M. S., and Baldwin, R. L. (1998). Alternative models for describing the acid unfolding of the apomyoglobin folding intermediate. *Biochemistry 37*, 7859−7868.
15. Antonini, E., and Brunori, M. (1971). in *Hemoglobin and myoglobin in their reactions with ligands*, American Elsevier, New York.
16. Pace, C. N. (1986). Determination and analysis of urea and guanidine hydrochloride denaturation curves. *Methods Enzymol. 131*, 266−280.
17. Santoro, M. M., and Bolen, D. W. (1988). Unfolding free energy changes determined by the linear extrapolation method. 1. Unfolding of phenylmethanesulfonyl α-chymotrypsin using different denaturants. *Biochemistry 27*, 8063−8068.
18. Johnson, C. M., and Fersht, A. R. (1995). Protein stability as a function of denaturant concentration: the thermal stability of barnase in the presence of urea. *Biochemistry 34*, 6795−6804.
19. Jamin, M., and Baldwin, R. L. (1998). Two forms of the pH 4 folding intermediate of apomyoglobin. *J. Mol. Biol. 276*, 491−504.
20. Takano, T. (1977). Structure of myoglobin refined at 2.0 Å resolution I. Crystallographic refinement of metmyoglobin from sperm whale. *J. Mol. Biol. 110*, 537−568.
21. Geierstanger, B. Jamin, M., Volkman, B. F., and Baldwin, R. L. (1998). Protonation behavior of histidine 24 and histidine 119 in forming the pH 4 folding intermediate of apomyoglobin. *Biochemistry 37*, 4254−4265.
22. Hargrove, M. S., and Olson, J. (1996). The stability of holomyoglobin is determined by heme affinity. *Biochemistry 35*, 11310−11318.
23. Shortle, D., and Meeker A. K. (1986). Mutant forms of staphylococcal nuclease with altered patterns of guanidine hydrochloride and urea denaturation. *Proteins 1*, 81−89.
24. Shortle, D. (1996). The denatured state (the other half of the folding equation) and its role in protein stability. *FASEB J 10*, 27−34.
25. Carra, J. H., and Privalov, P. L. (1996). Thermodynamics of denaturation of staphylococcal nuclease mutants: an intermediate state in protein folding. *FASEB J. 10*, 67−74.
26. Soulages, J. L. (1998). Chemical denaturation: potential impact of undetected intermediates in the free energy of unfolding and m-values obtained from a two-state assumption. *Biophys. J. 75*, 484−492.
27. Baskakov, I. V., & Bolen, D, W. (1998). Monitoring the sizes of denatured ensembles of staphylococcal nuclease proteins: implications regarding *m* values, intermediates, and thermodynamics. *Biochemistry 37*, 18010−18017.
28. Luo, Y., Kay, M. S., and Baldwin, R. L. (1997). Cooperativity of folding of the apomyoglobin pH 4 intermediate studied by glycine and proline mutations. *Nat. Struct. Biol. 4*, 925−930.
29. Kay, M. S., Ramos, C. H. I., and Baldwin, R. L, (1999). Specificity of nativelike interhelical hydrophobic contacts in the apomyoglobin intermediate. *Proc. Natl, Acad. Sci. U.S.A. 96*, 2007−2012.
30. Antosiewicz, J., McCammon, A., and Gilson, M. K. (1996). The determinants of pK_as in proteins. *Biochemistry 35*, 7819−7833.
31. Anderson, D. E., Becktel, W. J., and Dahlquist, F. W. (1990). pH-induced denaturation of proteins: a single salt bridge contributes 3−5 kcal/mol to the free energy of folding of T4 lysozyme. *Biochemistry 29*, 2403−2408.

32. Tissot, A. C., Vuilleumier, S., and Fersht, A. R. (1996). Importance of two buried salt bridges in the stability and folding pathway of barnase. *Biochemistry 35*, 6786−6794.
33. Waldburger, C. D., Schildbach, J. F., and Sauer, R. T. (1996). Are buried salt bridges important for protein stability and conformational specificity? *Nat. Struct. Biol. 2*, 122−128.
34. Spek, E. J., Bui, A. H., Lu, M., and Kallenbach, N. R. (1998). Surface salt bridges stabilize the GCN4 leucine zipper. *Protein Sci. 7*, 2431−2437.
35. Jaenicke, R. (1998). What ultrastable globular proteins teach us about protein stabilization. *Biochemistry (Moscow) 63*, 312−321.
36. Pace, C. N., Laurents, D. V. Thomson, J. A. (1990). pH dependence of the urea and guanidine hydrochloride denaturation of ribonuclease A and ribonuclease T1. *Biochemistry 29*, 2564−2572.
37. Yao, M, and Bolen, D, W. (1995). How valid are denaturant induced unfolding free energy measurements? Level of conformance to common assumptions over an extended range of ribonuclease A stability. *Biochemistry 34*, 3771−3781.
38. Anderson, D. E., Lu, J., McIntosh, L., and Dahlquist, F. W. (1993). The folding, stability and dynamics of T4 lysozyme: a perspective using nuclear magnetic resonance. in *NMR of proteins (Topics in molecular and structural biology)* (Clore, G. M., and Gronenborn, A. M., Eds.) pp 258−304, CRC Press, Boca Raton, FL.
39. Ibarra-Molero, B., Loladze, V. V., Makhatzdze, G. I., and Sanchez-Ruiz, J. M. (1999), Thermal versus guanidine-induced unfolding of ubiquitin. An analysis in terms of the contributions from charge−charge interactions to protein stability. *Biochemistry 38*, in press.

BI9828627